GeoHealth

Supporting Information for:

Next generation ice core technology reveals true minimum natural levels of lead (Pb) in the atmosphere: insights from the Black Death

Alexander F. More[1,2*], Nicole E. Spaulding[2], Pascal Bohleber[2,3], Michael J. Handley[2], Helene Hoffmann[3], Elena V. Korotkikh[2], Andrei V. Kurbatov[2], Christopher P. Loveluck[4], Sharon B. Sneed[2], Michael McCormick[1], Paul. A. Mayewski[2]

[1] Initiative for the Science of the Human Past and Department of History, Harvard University, 35 Quincy St., Cambridge, MA 02138, USA.
[2] Climate Change Institute, Sawyer Environmental Research Building, University of Maine, Orono, ME 04469, USA.
[3] Institute of Environmental Physics, Im Neuenheimer Feld 229, Heidelberg University, Heidelberg, D-69120, Germany.
[4] Department of Archaeology, University Park, School of Humanities, University of Nottingham, Nottingham NG7 2RD, UK.
* Corresponding author email: afmore@fas.harvard.edu

Contents of this file:

Additional Supporting Information (files uploaded separately)

Supporting data are included as Databases S1 and S2, and Datasets S3-S7 in SI files, listed below. Additional data may be obtained from AFM (afmore@fas.harvard.edu).

Database S1 Historical Geodatabase of Climate from Written Sources (ca. 1000-1425 C.E.)
Database S2 Historical Documentary Evidence of Epidemic Spread and Lead (Pb) Mining Activity (ca. 1340-1460 C.E.)
Dataset S3 Discrete ICP-MS Lead (Pb)
Dataset S4 LA-ICP-MS Calcium (ca. 1310-1317 C.E.)
Dataset S5 Enrichment Factors
Dataset S6 LA-ICP-MS Lead (Pb) (ca. 1300-1360 C.E.)
Dataset S7 Discrete ICP-MS Ca and Fe (ca. 1100-1600 C.E.)

5 Materials and Methods

Ice core data

The ice core studied in this paper was drilled to bedrock at Colle Gnifetti (Monte Rosa, 4450 m asl, Swiss-Italian Alps) in August of 2013. The drill site is located on the north-facing slope, on a flowline trending towards the eastern flank of the glacier. This site features a total ice thickness of around 72 m and a net surface accumulation of 20 cm of water equivalent per year. Following collection, the core was shipped to the Alfred Wegner Institute Helmholtz Center for Polar and Marine Research in Bremerhaven, where each section was cut into carefully co-registered sub-sections for further analysis at multiple laboratories.

We utilized the LA-ICP-MS system housed in the University of Maine Climate Change Institute's W. M. Keck Laser Ice Facility for the ultra-high resolution glaciochemical analysis presented in this study. Our methods follow those presented by *Sneed et al.*, (2015). Briefly, the components of this system include a Thermo Element 2 ICP-MS, a New Wave UP-213 laser, and a cryocell chamber, the Sayre Cell™, designed to seal a 1 m ice core from the surrounding air while maintaining a uniform temperature of −15°C. For complete operating parameters see Table S1.

Table S1. **LA-ICP-MS Operating Conditions.** Where two conditions are listed for a parameter the first refers to the single element method and the second to the multi-element method.

ICP-MS	Thermo Element 2
RF power	1300 W
Cooling gas	17.04 L/min
Auxiliary gas	0.9 L/min
Sample gas	0.75 L/min

LA-ICP-MS	New Wave UP-213
Carrier gas	1.2 L/min
Firing mode	continuous
Output level	100%
Repetition	10 Hz

		rate	
Additional gas	0.25 L/min	Spot size	100 μm
Element Masses	^{44}Ca; ^{208}Pb	Scan speed	85 μm/sec; 42 μm/sec
Resolution	Low; Medium	Fluence	31 J/cm^2
Scan Optimization	Accuracy; Speed		
Method Time	0.201 sec; 1.246 sec		

The sub-sections of the CG ice core used in this study are 25 mm X 85 mm semi-cylinders cut from the outside of a 98 mm diameter cylindrical ice core. Prior to analysis, the surface of the ice is scraped using a Lie Nielson stainless-steel blade to ensure a contaminant-free surface. The sample is then transferred into the Sayre Cell™ for analysis. ^{44}Ca was analyzed, as a single element within a single ablation track, for the lower 28 m of the ice core. Each sample represents a 117 μm depth increment (the width of the laser beam, plus the distance traversed during a single ICP-MS scan of 0.201 seconds at 85 μm/sec). ^{208}Pb was analyzed for the time period encompassing the Black Death as part of a multi-element (five) suite within a single ablation track. Increasing the number of elements analyzed within a single track increases the duration of a single ICP-MS scan to, in this case, 1.246 seconds, thereby reducing the resolution. To minimize this reduction, the scan speed of the laser was also reduced to 42.5 μm/sec. The subsequent resolution is 153 μm. An airtight seal over the ice is required by the laser ablation system for the argon carrier gas to transfer the ablated ice material into the ICP-MS, thus gaps exist in the record where individual sections (~1 m in length) of the CG ice core were separated during extraction from the glacier. To calculate glaciochemical concentrations from intensities as measured by LA-ICP-MS, a calibration technique using both liquid and frozen standards is used, as in *Sneed et. al*. (2015).

Discrete ICP-MS aliquots were sampled from the meltwater produced during the continuous flow analysis of the CG core at the Institute for Climate and Environmental Physics, at the University of Bern in Bern, Switzerland [*Kauffman et al.*, 2008, *Osterberg et al.*, 2006]. Samples were split for subsequent analysis by ion chromatography and ICP-MS in the Climate Change Instituite's laboratories. ICP-MS samples were acidified to 1% with double-distilled HNO_3 under a class-100 HEPA clean bench and allowed to react with the acid for approximately 14 days before analysis. The acidified samples were then analyzed following the procedure and detection limits outlined in *Osterberg et al.,* (2006). Briefly, analyses were performed with a Thermo Electron Element2 ICP-MS. A series of isotopes were measured, though only ^{44}Ca (medium resolution) and ^{208}Pb (low resolution) are reported here. An ESI Apex high-sensitivity inlet system was used to increase sensitivity and reduce oxide formation in the plasma thereby lowering detection limits. The ICP-MS is calibrated daily with five standards that bracket the expected sample concentration range and certified water reference material, SLRS-4 (Environment Canada), is used to verify the calibration.

The measurements for radiocarbon dating of the ice core were conducted at the Institute of Environmental Physics (Heidelberg, Germany) under close collaboration with the AMS facility at the Klaus-Tschira-Lab in Mannheim, Germany. The microscopic particulate organic carbon fraction (POC) incorporated into the ice matrix was extracted, combusted and analyzed for ^{14}C content. Calibration of the retrieved ages was performed using OxCal version 2.4 (*Bronk Ramsey*, 1995). For details on the sample preparation and measurement procedure see *Hoffmann*, 2016.

Crustal Enrichment Factor values (EF_c) were calculated to estimate contributions for Pb from crustal dust sources using the following equation:

$$EF_c\ (X)=(X/Ti)_{sample}/(X/Ti)_{UCC}$$

where X is an element of interest, Ti is used as a crustal reference element, and upper continental crust (UCC) values were obtained from *Wedepohl et al.*, (1995). Ti rather than Al concentrations in UCC is used here to mitigate the potential risk of contamination during ice drilling, since most ice-core drill components are made of Al. To investigate any volcanic sources of Pb we made a radical estimation that 10% of the total S in Colle Gnifetti ice is of volcanic origin, and calculated EF_v using the following equation:

$$EF_v\ (X)=[X/(10\%\ \text{of}\ S)]_{sample}/[X/S]_{worldwide\ volcanic\ emission}$$

Where the ratio of X (measured element) to measured 10% S concentrations is normalized to the ratio of the same element in the crust to S from estimates of global volcanic emissions from *Hinkley et al.*, (1999).

All impurity species measured by CFA were used in combination for annual layer counting. Annual layers were defined as local maxima in at least two impurity species, with special emphasis on NH4+ featuring the largest seasonal amplitude. An independent counting was performed using the LA-ICP-MS Ca profile starting at 29.5 m WE (corresponding to 1760 AD). At this depth, the average annual layer thickness was estimated from CFA-based counting as around 3 cm. For the depth interval 29.5-32.5 m WE, counting in the LA-ICP-MS Ca record results in good agreement with counting performed on the CFA profile (typically within +/- 1 year per 10 counted years). Below 32.5 m WE, average annual layer thickness becomes close to 1 cm and counting in the CFA profile becomes increasingly difficult. Accordingly, LA-ICP-MS Ca was the dominant source of annual layer counting after around 32.5 m WE (1600 AD).

We estimated the dating uncertainty from the above annual layer counting procedure through quantifying the likelihood of miscounting layers by marking “uncertain years.” For instance, uncertain layers were defined as additional peaks in close proximity to an annual layer (e.g. “shoulder type” peaks). To quantify counting uncertainty from uncertain layers, we followed the approach successfully employed at Greenland ice cores. This is to count uncertain layers as 0.5+/-0.5 years and to estimate the maximum counting error (MCE) from N uncertain layers as N x 0.5 years [*Andersen et al.*, 2006; *Rasmussen et al.*, 2006]. With 144 uncertain layers detected within the upper 40 m WE of KCC, this corresponds to an uncertainty of +/- 72 years around 1000 years BP.

A review was also undertaken of the peat and lake sediment cores across western and central Europe and Scandinavia for evidence of comparative trends (although at lower chronological resolution than the CG ice core). The publications of the most chronologically reliable cores, with large numbers of radiocarbon dates informing their age-depth models, are cited in the text. Future publications of the "Historical Ice Core Project" that make greater use of the geoarchaeological records to inform interpretation of the CG ice core will collate these records and make them available in open access to the public, through the website of the Initiative for the Science of the Human Past.

Historical data

All historical data pertaining to epidemics, their extent and date of arrival in different regions of Europe was collected independently of the ice-core datasets. Primary sources consisted of legal and fiscal records as well as chronicles. The dates of arrival and spread of epidemic (in most cases *Yersinia pestis*) in each cited location was recorded in Table S2, database 2 (submitted with this article), and summarized in Table 1. On rare occasions, when dates included the month of the epidemic's arrival and the authors of secondary sources consulted did not adjust years to modern calendar dates (beginning the new year on January 1st), this adjustment was effected a posteriori. Similarly, data pertaining to mining and smelting activities throughout Europe was collected from primary and secondary sources, cited in the main text as well as in Tables S3, S4 and S5 and more extensively in Database 2.

Historical reports of climate data were assembled from primary and secondary sources, independently of the ice-core data; in all cases, each report provides the primary source from which it originates. Dates provided in all historical tables and databases are limited to year and month, when the latter was available. The uncertainty in each record is limited only by the information supplied by each historical report. Each report was checked for accuracy with multiple secondary sources. For all historical evidence of epidemic arrival and spread, or mining activity, and for most climate reports, multiple independent historical reports corroborate our identification of a single event or trend.

The database of climate reports used for this article, as well as future versions thereof, are available in the public domain, by accessing the website of the Initiative for the Science of the Human Past at Harvard, as well as the *Digital Atlas of Roman and Medieval Civilization* and the Harvard Dataverse dedicated to the “Historical Ice Core Project” of the Initiative for the Science of the Human Past. In the latter repository, each database version, including the one used for this article, have a unique Digital Object Identifiers.

SI Figures

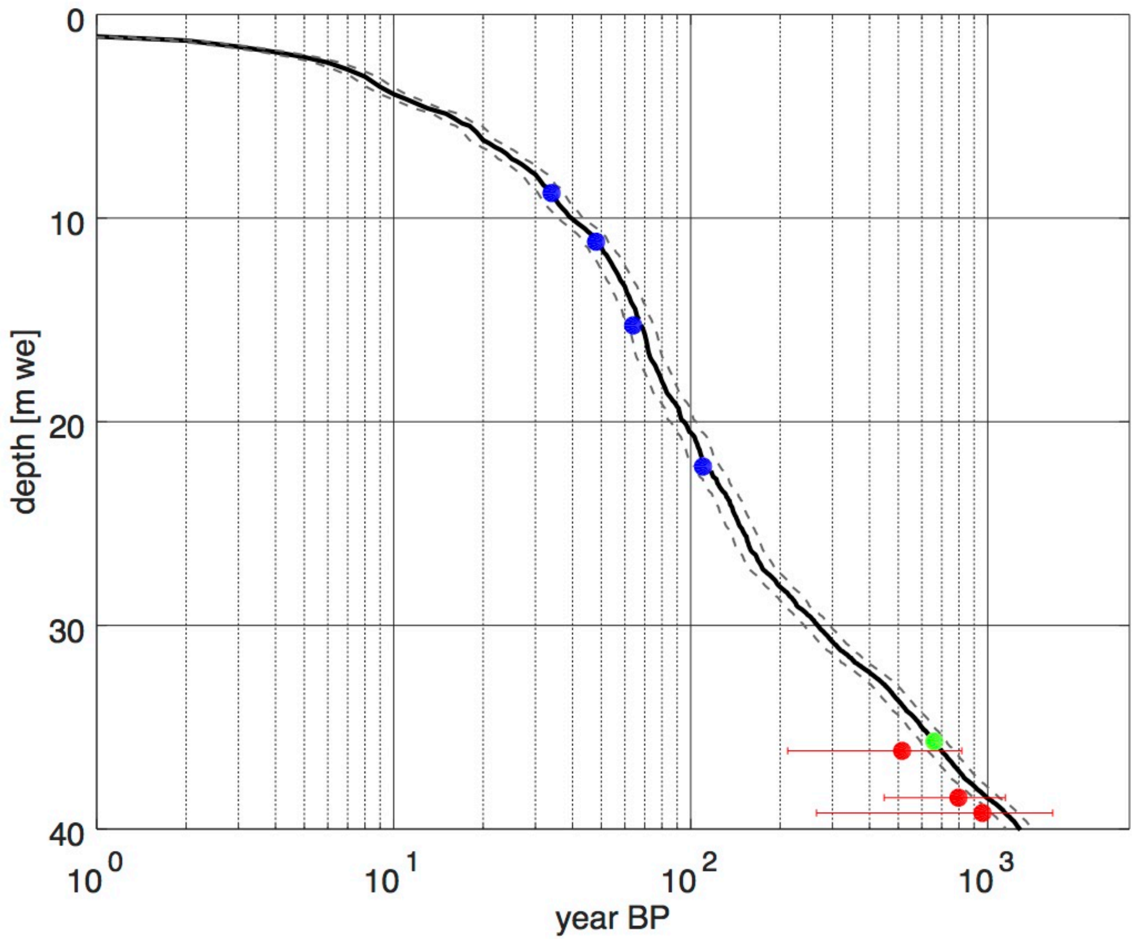

Fig. S1. Age-depth scale of the Colle Gnifetti ice core, based on annual layer counting (in black, with a 10% uncertainty envelope of the MCE error visualized as grey dashed lines). Also shown in blue are absolute age horizons used to check counting accuracy (known dust falls and the 3H horizon). Micro-^{14}C dating is shown as red dots with a 1σ error bars. The green dot shows the location of the Pb Black Death anomaly. Note that the total core depth is approx. 54 m we.

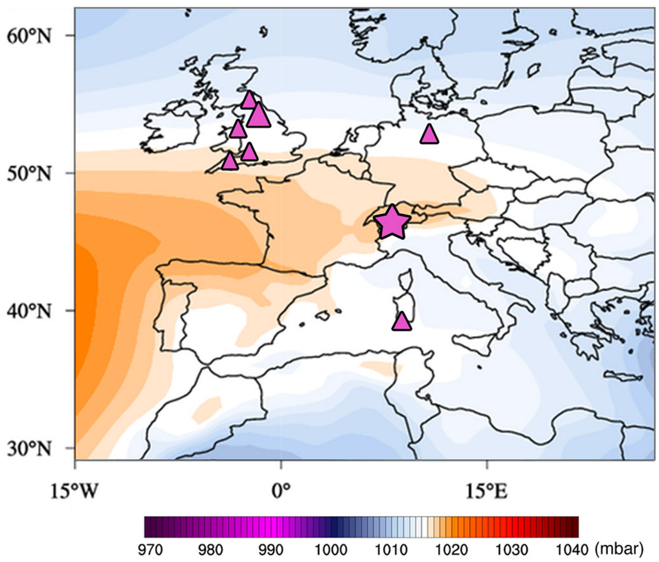

193

Figure S2 | Summer mean sea level pressure (mbar) example of the "reach" of the Azores High pressure system. The figure shows atmospheric circulation (ERA-Interim reanalysis plotted using CCI-Climate Reanalyzer), transporting air masses clockwise from the major Pb/Ag mining centers (▲) of the 1347-1460C.E. era to CG (★). Size of triangles indicates approximate volume of production determined from written records.

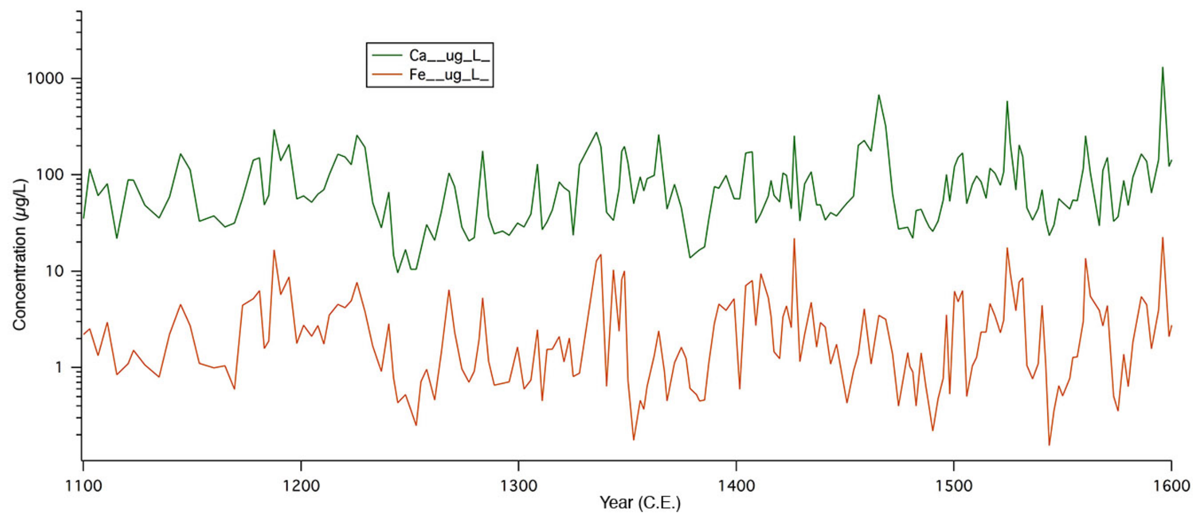

Fig. S3. No evidence of atmospheric circulation change at time of Black Death. Lack of anomalous average Ca and Fe, proxies for crustal air masses, in the years 1349-1353C.E. Circulation and climate patterns were further corroborated by comparison with SoHP Historical Geodatabase of Climate Events (Supplementary Data 5).

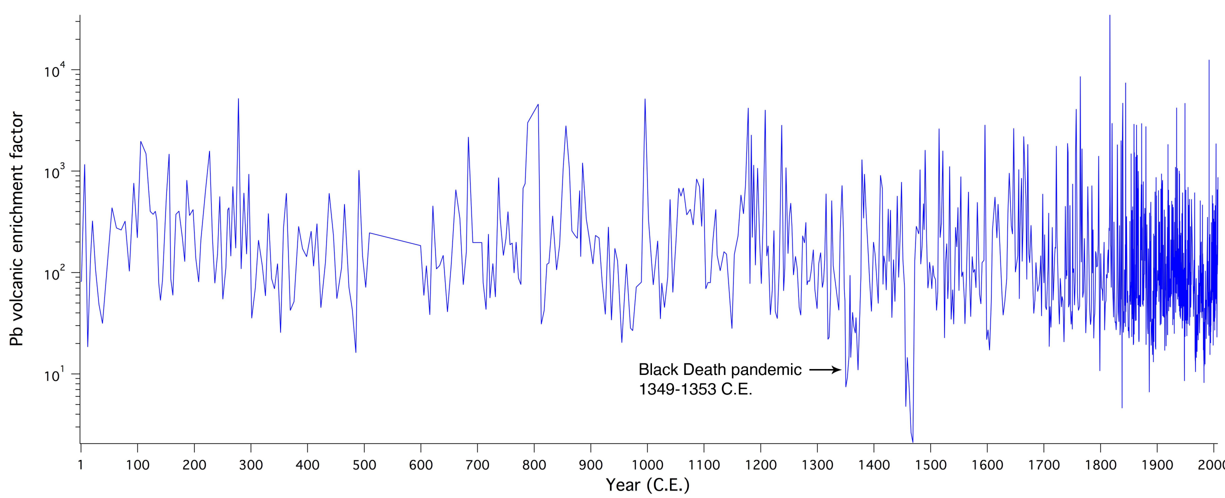

Fig. S4. Pb volcanic enrichment factor (EF_v). The volcanic enrichment factor calculations (using Hinkley et al., 1999 dataset) are shown above. The graph covers the period 1 C.E-2007C.E. The Black Death drop marks the years 1349-1353C.E. Values below 10 here are based on semi-quantitative calibration data.

SI Tables

Table S2. Arrival dates of the Black Death and later epidemic outbreaks in major mining regions of Europe.

Region	Date epidemic arrives
Britain	
Mendip (SW England) (1-8)	1348/1349
Devon (Bere Ferrers, SW England) (3, 9)	1349 March
Derbyshire (Peak District, Central England) (10-11)	1349 May
Flintshire (North Wales) (10)	1349 April-June
East Riding/Humberside, Yorkshire (York, Hull, NE England) (8)	1349 May
Lancashire (7)	1349
Cheshire (13)	1349 June
Nottingham (Central England) (7)	1349
Newcastle (14-15)	1349 June-Aug
Durham (Weardale, NE England) (15)	1349 June-Aug
England (all) (16)	1447-54
England (all) (16-17)	1462-3
England (all) (7, 16-18)	1464-5 Oct
Germany	
Harz (Halberstadt) (4-15)	1350 May
Magdeburg (15)	1350 May
Italy	
Sardinia (Iglesias) (19)	1348

Table S3. Dates in which mining activities are documented to have ceased.

Region	Date mining activities cease
Britain	
Mendip (20)	1340s
Devon (Bere Ferrers) (20)	1349
Derbyshire (Peak District) (20)	1349-52
Flintshire (20)	1349-50
Derbyshire (Peak District) (20)	1460-1
Mendip (20)	1460
Durham (Weardale, new mine) (20)	1460
W Yorkshire (Nidderdale, Arkengarthdale, Wensleydale) (58)	1457-64
Germany	
Harz (20)	1350
Goslar (21)	1350

Table S4. Revival or new activity in major mining regions of Europe.

Region	Year of revival or new mining activity
Britain	
W Yorkshire (Nidderdale) (20)	1352
Derbyshire (High Peak) (20)	1352
Flintshire (N Wales) (20)	1354
Mendip (20)	1360
Yorkshire (remainder) (20)	1360
Italy	
Sardinia (Iglesias) (19)	1420
Germany	
Harz (22)	1460s

Table S5. Peak District (Derbyshire) lead (Pb) tithes. Value (in pounds) is linked to main mines pre- and post-Black Death. The collapse in value of the returns from particularly well documented mines reveals the dramatic scale of the drop in production, as a result of the spread of the Black Death and resulting cessation of mining activities. (20)

Mine	Value pre-Black Death	Value Post-Black Death (£)
Ashford	£20 (1348C.E.)	£1 (1353C.E.)
Youlgreave	£50 (1348C.E.)	0 (1349C.E.)
Bakewell	£18 (1342C.E.)	£10 (1356C.E.)

SI Table References

1. Babington, C., J. R. Lumby, eds. (1882) *Polychronicon Ranulphi Higden Monachi Cestrensis*, Rolls Series, 41.8. (London, UK, Longman): 355.
2. Galbraith, V. H., ed. (1970) *The Anonimalle Chronicle*. (Manchester, UK, Manchester Univ. Press): 30.
3. Horrox, R. (1970) *The Black Death* (Manchester, UK, Manchester Univ. Press): 62-63, 81, 275.
4. Sticker, G. (1908-10) *Abhandlungen aus der Seuchengeschichte und Seuchenlehre: Geschichte der Pest* (Giessen, Töpelmann) 1: 69, 68.
5. Benedictow, O.J. (2004), *The Black Death, 1346-1353: The Complete History* (Rochester, NY, Boydell): 128, 195-6.
6. Gottfried, R.S. (1989), Plague, Public Health and Medicine in Late Medieval England, in *Maladie et société (XII^{e}-XVIII^{e} siècles)* eds Bulst N, Delort R (Paris, CNRS): 337-65.
7. Creighton, C. (1891), *A History of Epidemics in Britain* (Cambridge, UK, Cambridge Univ. Press) vol. 1: 116, 118, 134, 138, 230.
8. Thompson, E. M. ed. (1889), *Chronicon Galfridi le Baker de Swynebroke* (Oxford, UK, Clarendon Press): 99.
9. Public Record Office, London, *Exchequer plea rolls*, E 13/77 (membrane 40).
10. Cox, J. C. (1875), *Notes on the Churches of Derbyshire*, (London, UK, Bemrose) vol. 4: vii.
11. Davies, R. A. (1989), The effect of the Black Death on the parish priests of the medieval diocese of Coventry and Lichfield. *Historical Research* 62(147): 85-90.
12. Rees, W. (1920), The Black Death in Wales. *Transactions of the Royal Historical Society* 3:115-35.
13. Ormrod, W. M. and P. Lindley (1996), *The Black Death in England, 1348-1500*. (Stamford, UK, Watkins): 22.
14. Gasquet, F. A. (1908), *The Black Death of 1348 and 1349* (London, UK, Bell): 185-6.

15. Thompson, A. H. (1914), The pestilences of the fourteenth century in the diocese of York. *Archaeological Journal* 71(1): 97-154.
16. Shrewsbury, J. F. D. (1970), *A history of bubonic plague in the British Isles* (Cambridge, UK, Cambridge Univ. Press): 145, 147.
17. Gottfried, R. S. (1978), *Epidemic disease in fifteenth-century England* (New Brunswick, NJ, Rutgers Univ. Press): 41-2.
18. Brown, R. ed. (1864), *Calendar of State Papers and Manuscripts Relating to English Affairs: Venice* (London, UK, Longman) vol. 1: 114.
19. Anatra, B. (1989), Economia sarda e commercio mediterraneo nel basso medio evo e nell'età moderna. *Storia dei Sardi e della Sardegna*, ed Guidetti M (Milan, Jaca): 109-216.
20. Blanchard, I. (2005), *Mining, Metallurgy and Minting in the Middle Ages*, (Stuttgart, Germany, Steiner) vol. 3: 1406-7, 1693-5, 1697, 1623, 1372, 1381, 1376, 1392, 1481, 1360-2, 1394, 1464, 1460, 1492, 1398, 1371-2, 1407, 1425, 1383-4, 1388-92, 1425, 1392-4, 1372.
21. Bartels, C. (1996), Mittelalterlicher und frühneuzeitlicher Bergbau im Harz und seine Einflüsse auf die Umwelt. *Natur & Wissenschaften* 83(11): 483-91.
22. Bartels, C. (2010), The production of silver, copper, and lead in the Harz mountains from late medieval times to the onset of industrialization. *Materials and Expertise in Early Modern Europe*, U. Klein, E. C. Spary eds. (Chicago, Univ. of Chicago Press): 71-100.